Am J Physiol Endocrinol Metab 306: E1077–E1084, 2014.
First published March 11, 2014; doi:10.1152/ajpendo.00659.2013.

CXCL1/CXCL8 (GROα/IL-8) in human diabetic ketoacidosis plasma facilitates leukocyte recruitment to cerebrovascular endothelium in vitro

Tatsushi Omatsu,[1–3] Gediminas Cepinskas,[1,4] Cheril Clarson,[2,3] Eric K. Patterson,[1] Ibrahim M. Alharfi,[5] Kelly Summers,[6] Pierre-Olivier Couraud,[7–9] Ignacio A. Romero,[10] Babette Weksler,[11] and Douglas D. Fraser[1–3,12–14] (On Behalf of the Canadian Critical Care Translational Biology Group)

[1]*Centre for Critical Illness Research, London, Ontario, Canada;* [2]*Children's Health Research Institute, London, Ontario, Canada;* [3]*Department of Paediatrics, Western University, London, Ontario, Canada;* [4]*Department of Medical Biophysics, Western University, London, Ontario, Canada;* [5]*Department of Pediatric Critical Care, King Fahad Medical City, Riyadh, Saudi Arabia;* [6]*Department of Microbiology and Immunology, Western University, London, Ontario, Canada;* [7]*Institut National de la Sante et de la Recherche Medicale, U1016, Institut Cochin, Paris, France;* [8]*Centre National de la Recherche Scientifique, UMR8104, Paris, France;* [9]*Université Paris Descartes, Sorbonne Paris Cité, Paris, France;* [10]*Biomedical Research Network, The Open University, Milton Keynes, United Kingdom;* [11]*Department of Medicine, Weill Cornell Medical College, New York, New York;* [12]*Department of Physiology and Pharmacology, Western University, London, Ontario, Canada;* [13]*Department of Clinical Neurological Sciences, Western University, London, Ontario, Canada; and* [14]*Translational Research Centre, London, Ontario, Canada*

Submitted 2 December 2013; accepted in final form 4 March 2014

Omatsu T, Cepinskas G, Clarson C, Patterson EK, Alharfi IM, Summers K, Couraud PO, Romero IA, Weksler B, Fraser DD (On Behalf of the Canadian Critical Care Translational Biology Group). CXCL1/CXCL8 (GROα/IL-8) in human diabetic ketoacidosis plasma facilitates leukocyte recruitment to cerebrovascular endothelium in vitro. *Am J Physiol Endocrinol Metab* 306: E1077–E1084, 2014. First published March 11, 2014; doi:10.1152/ajpendo.00659.2013.—Diabetic ketoacidosis (DKA) in children is associated with intracranial vascular complications, possibly due to leukocyte-endothelial interactions. Our aim was to determine whether DKA-induced inflammation promoted leukocyte adhesion to activated human cerebrovascular endothelium. Plasma was obtained from children with type 1 diabetes either in acute DKA or in an insulin-controlled state (CON). Plasma concentrations of 21 inflammatory analytes were compared between groups. DKA was associated with altered circulating levels of ↑CXCL1 (GROα), ↑CXCL8 (IL-8), ↑IL-6, ↑IFNα2, and ↓CXCL10 (IP-10) compared with CON. These plasma analyte measurements were then used to create physiologically relevant cytokine mixtures (CM). Human cerebral microvascular endothelial cells (hCMEC/D3) were stimulated with either plasma (DKA-P or CON-P) or CM (DKA-CM or CON-CM) and assessed for polymorphonuclear leukocyte (PMN) adhesion. Stimulation of hCMEC/D3 with DKA-P or DKA-CM increased PMN adhesion to hCMEC/D3 under "flow" conditions. PMN adhesion to hCMEC/D3 was suppressed with neutralizing antibodies to CXCL1/CXCL8 or their hCMEC/D3 receptors CXCR1/CXCR2. DKA-P, but not DKA-CM, initiated oxidative stress in hCMEC/D3. Expression of ICAM-1, VCAM-1, and E-selectin were unaltered on hCMEC/D3 by either DKA-P or DKA-CM. In summary, DKA elicits inflammation in children associated with changes in circulating cytokines/chemokines. Increased CXCL1/CXCL8 instigated PMN adhesion to hCMEC/D3, possibly contributing to DKA-associated intracranial vascular complications.

CXC chemokine ligand; growth-regulated oncogene-α; human; pediatric; diabetes; ketoacidosis; brain; cell trafficking; neutrophils; chemokines; inflammation

THE INCIDENCE OF TYPE 1 DIABETES has been increasing in children, nearly doubling in the last decade (42). A frequent complication of type-1 diabetes is diabetic ketoacidosis (DKA), a state of severe insulin deficiency resulting in hyperglycemia, ketonemia, and metabolic acidosis (5). Potential consequences of DKA in children include cerebral hemorrhage (32, 34), stroke (12, 40), and vasogenic edema (11, 15, 24), suggesting cerebrovascular dysfunction.

DKA is an inflammatory state with acute systemic elevations in heat shock proteins (35), complement (25), activated lymphocytes (22), and cytokines (20, 27). Acute inflammation from other pathologies (i.e., infection, ischemia, or trauma) activates both endothelial cells and leukocytes, resulting in increased endothelial-leukocyte adhesion (7). Leukocytes adhered to the endothelium produce and release reactive oxygen species (ROS), proteases, cationic proteins, and other substances that injure microvessels (16).

Recently, we demonstrated that DKA elicits systemic inflammation associated with cerebrovascular endothelial dysfunction in a juvenile mouse model (6); however, pancreatic toxins were required to instigate acute DKA and may have contributed to the systemic inflammation (41). Thus, the aims of this study were to characterize the acute inflammatory state in children with DKA and to determine whether DKA-induced inflammation can result in increased cerebrovascular endothelial-leukocyte adhesion in human tissues.

MATERIALS AND METHODS

This study was approved by the Health Sciences Research Ethics Board at Western University. Patient recruitment took place in our regional tertiary care centre at The Children's Hospital, London Health Sciences Centre (London, ON, Canada).

Human subjects. Consent was obtained from the legal guardians of all pediatric patients admitted with DKA, and both legal guardian consent and patient assent were obtained for type 1 diabetes control patients. Biochemical diagnostic criteria for DKA included hyperglycemia >11 mmol/l, bicarbonate <15 mmol/l, and ketonurea (9). DKA is classed according to severity of acidosis as mild (venous pH < 7.3), moderate (pH < 7.2), or severe DKA (pH < 7.1) (4, 38). Only severe or moderate DKA cases were used in this study. Clinic patients with

Address for reprint requests and other correspondence: D. D. Fraser, Paediatric Critical Care Medicine, Rm. No. C2-846, Children's Hospital, London Health Sciences Centre, 800 Commissioners Rd. East, London, Ontario, Canada, N6A 5W9 (e-mail: douglas.fraser@lhsc.on.ca).

controlled type 1 diabetes ($A_{1C} < 10\%$ and no DKA for 3 mo) served as controls.

Blood collection and processing. Blood for research purposes was obtained on hospital presentation at the time of clinically indicated blood draws. Blood was drawn into citrate-containing tubes (Vacutainers; BD Biosciences, Mississauga, ON, Canada) by certified nursing personnel, placed on ice, and immediately transferred to the Translational Research Centre facility for processing by standard operating procedures (www.translationalresearch.ca; London, ON, Canada) (1, 14). Briefly, blood was centrifuged at 1,500 *g* for 15 min (4°C), and the upper plasma layer was collected in 250-μl aliquots and frozen at −80°C. Thawed plasma was maintained on ice for short periods prior to use in experiments, and freeze-thaw cycles were avoided.

Human plasma inflammatory protein analysis. The concentrations of 21 plasma cytokines/chemokines and soluble adhesion markers were measured: interleukin (IL)-1β, IL-2, IL-6, IL-10, IL-17, interferon-α2 (IFNα2), interferon-γ (IFNγ), granulocyte macrophage colony-stimulating factor (GM-CSF), granulocyte colony-stimulating factor (G-CSF), vascular endothelial growth factor (VEGF), CXC chemokine ligand 1 [CXCL1, growth-regulated oncogene-α (GROα)], CXCL8 (IL-8), CXCL10 [interferon-γ-induced protein-10 (IP-10)], CC chemokine ligand 2 (CCL2; monocyte chemoattractant protein-1), CCL3 [macrophage inflammatory protein (MIP)-1α], CCL4 (MIP-1β), tumor necrosis factor-α (TNFα), soluble cluster of differentiation 40 ligand (sCD40L), soluble endothelium-selectin (sE-selectin), soluble intercellular adhesion molecule-1 (sICAM-1), and soluble vascular cell adhesion molecule-1 (sVCAM-1). Concentrations of analytes were determined with multiplexed immunoassay kits and a Bio-Plex 200 readout System (Bio-Rad Laboratories, Hercules, CA), which utilizes Luminex xMAP fluorescent bead-based technology (Luminex). Levels were automatically calculated from standard curves using Bio-Plex Manager software (version 4.1.1; Bio-Rad Laboratories, Hercules, CA).

Human cerebral microvascular endothelial cells. The human cerebral microvascular endothelial cell line (hCMEC/D3) (49) was used as a model of brain microvascular endothelium in vitro. The hCMEC/D3 cell line offers an ideal opportunity to study human cerebrovascular cells in isolation from other cells and represents a stable, fully characterized, and well-differentiated human brain endothelial cell line (48). hCMEC/D3 cells were cultured in VascuLife basal medium (VL; Lifeline Cell Technology) supplemented with VascuLife EnGS-Mv LifeFactor Kit (Lifeline Cell Technology), 100 IU/ml penicillin, and 100 μg/ml streptomycin (Wisent) on collagen I-coated plates (100 μg/ml in water; Sigma-Aldrich). The cells were maintained at 37°C in a humidified atmosphere with 5% CO_2 and reseeded when the cell monolayer became subconfluent. hCMEC/D3 at passages 35–45 was used in all experiments.

In vitro experimental approach. hCMEC/D3 cells were stimulated with either DKA (DKA-P) or control (CON-P) plasma at a concentration of 20% (vol/vol) and diluted in VL medium containing 1 U/ml heparin (Pharmaceutical Partners of Canada). A final plasma concentration of 20% produced near-maximal cellular responses in sepsis experiments (18), and the use of higher plasma concentrations was precluded by plasma coagulation and detachment of the cell monolayer from the underlying membrane. The media pH was unchanged by the 20% plasma dilutions (DKA-P, 7.40 ± 0.06 vs. CON-P, 7.42 ± 0.06; $P = 0.852$).

Based on the plasma measurements of cytokines/chemokines presented in Table 2, and using $P < 0.01$ to control for repeated measurements, two cytokine mixtures (CM) of the same five recombinant human cytokines/chemokines that contained equivalent concentrations measured in human DKA-P (DKA-CM) and CON-P (CON-CM) were prepared. The CM consisted of human purified IL-6, CXCL1, CXCL8, CXCL10, and IFNα2 (Life Technologies). The 100× cytomix stock solutions were prepared in phosphate-buffered saline (PBS) containing 0.1% bovine serum albumin (BSA). For experiments, each cytomix stock solution was diluted in VL medium. The final concentration of each cytomix was as follows: CON-CM: CXCL1 (94 pg/ml), CXCL8 (9 pg/ml), CXCL10 (525 pg/ml), IL-6 (4 pg/ml), and IFNα2 (29 pg/ml); DKA-CM: CXCL1 (204 pg/ml), CXCL8 (44 pg/ml), CXCL10 (169 pg/ml), IL-6 (22 pg/ml), and IFNα2 (70 pg/ml).

Purified interference antibodies. Anti-human CXCL1/CXCL8 antibodies (R & D Systems) were used at 1 μg/ml concentration in plasma or cytomix for 15 min to neutralize CXCL1/CXCL8. Mouse IgG_1 (BioLegend) was used for their isotype control. Anti-human CXC chemokine receptor antibodies against CXCR1/CXCR2 (R & D Systems) were applied at a concentration of 1 μg/ml for 30 min prior to plasma or cytomix stimulation. Mouse IgG_{2A} (R & D Systems) was used for their isotype control.

Oxidative stress. Oxidative stress in hCMEC/D3 cells was assayed by intracellular oxidation of dihydrorhodamine 123 (DHR123; Molecular Probes), an oxidant-sensitive fluorochrome, as described previously (2). hCMEC/D3 cells were incubated with 10 μM DHR123 for 45 min prior to stimulation. Following the 1-h stimulation of CON-/DKA-P or CON-/DKA-CM, cells were washed with PBS and subsequently incubated on ice for 10 min with 0.1% CHAPS solution (with 50 mM K_2HPO_4, 20 mM EDTA). The cells were then scraped and sonicated. The lysates were centrifuged at 20,000 *g* for 10 min at 4°C, and then the supernatants were used for fluorescent assay. The level of DHR123 oxidation was determined spectrofluorometrically (RF-1501 Spectrophotometer; Shimadzu) using excitation and emission wavelengths of 502 and 523 nm, respectively. DHR123 oxidation was expressed as fluorescence emission per microgram of protein. The lysate protein concentration was quantified using the Bio-Rad Protein Assay (Bio-Rad Laboratories).

Transendothelial electrical resistance. The permeability of the hCMEC/D3 monolayer was determined by transendothelial electrical resistance (TEER). hCMEC/D3 cells were grown on Transwell inserts with 0.4-μm pore size membranes (BD Biosciences). Subsequently, the confluent hCMEC/D3 monolayers were exposed to 20% CON-P or DKA-P, and TEER (Ω) was recorded at multiple time points (0–120 min) by using an EVOM2 voltohmmeter equipped with the Endohm-6 chamber (World Precision Instruments). TEER measurements are presented as a percent change from the initial monolayer baseline resistance.

Polymorphonuclear leukocyte adhesion assay. Human polymorphonuclear leukocytes (PMNs) were freshly isolated from venous blood of healthy volunteers using standard dextran sedimentation and gradient separation on Histopaque-1077 (Sigma-Aldrich). This procedure yields a PMN population that is 95–98% viable (trypan blue exclusion) and 98% pure (acetic acid crystal violet staining) (3). Isolated PMNs were resuspended in PBS at 3×10^7 PMN/ml and subsequently incubated at room temperature for 10 min before perfusion. hCMEC/D3 cells were grown to confluence in μ-Slide $VI^{0.4}$ channels (IBIDI) and stimulated with CON-/DKA-P or CON-/DKA-CM for 6 h. The cell monolayers were then perfused with VL medium with 4% FBS at a shear stress of 0.35 dyn/cm^2 for 1 min (6). Subsequently and continuously, PMNs (1×10^6 cells/ml in VL medium with 4% FBS) were perfused over the cell monolayers for 10 min in the presence of 0.35 dyn/cm^2 shear stress. All experimental procedures were performed at 37°C using a Nikon Diophot300 inverted microscope (Nikon) equipped with a temperature-controlled chamber and SONY CCD Iris Video Camera DXC-107A (Sony) connected to a HD PVR-video recorder (Hauppauge Computer Works) and recorded (MP4 format) for later analyses. PMN adhesion (reaining stationary for ≥10 s) was counted after 5-min PMN perfusion in five separate randomly chosen areas and expressed as the average number of cells per 0.1 mm^2.

Reverse transcription quantitative PCR. Expression of adhesion molecule mRNAs in hCMEC/D3 cells were quantified using PCR. One-step RT-qPCR was performed for CON/DKA-plasma stimulated cells, whereas a two-step method was performed for CON/DKA-

Table 1. *Human clinical and biochemical data for CON and DKA type 1 diabetes patients*

	CON	DKA	*P* Value
Age, yr	11.6 ± 1.3	11.9 ± 0.9	0.847
Sex (boys%)	6/10 (60%)	6/10 (60%)	1.000
A_{1C} (%)	8.7 ± 0.4	11.7 ± 0.8	**0.003**
pH	NA	7.1 ± 0.1	
HCO_3^-, mmol/l	NA	7.9 ± 1.9	

Values are means ± SE; $n = 10$. CON, insulin controlled; DKA, patients with an acute ketoacidosis episode; NA, not available. Blood gases were not performed on CON patients. Boldface indicates significant *P* value.

cytomix stimulated cells. As a one-step method, total RNA was isolated by using iScript RT-qPCR Sample Preparation Reagent (Bio-Rad) according to the manufacturer's suggested protocol from hCMEC/D3 cells stimulated for 4 h with CON or DKA plasma or VL medium alone as a negative control. Subsequently, the iScript One-Step RT-PCR Kit For Probes (Bio-Rad) was used according to the manufacturer's suggested protocol. As a two-step method, total RNA was isolated by using TRIzol Reagent (Invitrogen) according to the manufacturer's suggested protocol from hCMEC/D3 cells stimulated for 4 h with CON or DKA cytomix or VL medium alone as a negative control. A 1-μg aliquot of total RNA was reverse transcribed into cDNA with a Px2 Thermal Cycler (Thermo Scientific) using iScript Reverse Transcription Supermix for RT-qPCR (Bio-Rad). SsoFast Probes Supermix (Bio-Rad) was then used according to the manufacturer's suggested protocol. Predesigned gene-specific TaqMan Gene Expression Assay primers (Applied Biosystems) were used for qPCR. Every set contained gene-specific forward and reverse primers and fluorescence-labeled probes. These assay IDs were CAM-1, Hs00164932_m1; VCAM-1, Hs01003372_m1; E-selectin, Hs00950401_m1; and 18s rRNA, Hs99999901_s1. Real-time PCR was carried out with the CFX96 Real-Time PCR Detection System-IVD (Bio-Rad). The PCR settings were as follows: 5-min initial denaturation at 95°C and 55 cycles of 15-s denaturation at 95°C, 45-s annealing, and extension at 60°C for the one-step method; 30-s initial denaturation at 95°C and 55 cycles of 5-s denaturation at 95°C, 15-s annealing, and extension at 60°C for the two-step method. Quantification of gene expression was calculated relative to 18s rRNA expression.

Statistical analysis. Data are presented as means ± SE. Statistical significance ($P < 0.05$) was assessed with the Excel 2007 (Microsoft) add-in software Ekuseru-Toukei 2008 (Social Survey Research Information). All data were prescreened for normality with the Kolmogorov-Smirnov test and then assessed using either an unpaired *t*-test when the data were normally distributed or a Mann-Whitney *U*-test when the data were skewed.

RESULTS

Study patients. Plasma was obtained from type 1 diabetes patients either in acute DKA or in an insulin-controlled state. The two groups were age and sex matched ($n = 10$ patients/group; Table 1). Patients with DKA had significantly higher A_{1C} values compared with those with controlled type 1 diabetes ($P = 0.003$), reflecting elevated blood glucose over the preceding few months. DKA patients all had moderate to severe metabolic acidosis.

Plasma inflammatory analytes. The levels of inflammatory cytokines and soluble adhesion molecules were measured in plasma from both DKA and CON groups (Table 2; $n = 10$ patients/group). Out of the 18 cytokines/chemokines assessed, six (CXCL1, CXCL8, IL-6, IFNα2, IL-2, and G-CSF) were found to be significantly increased, and one (CXCL10) was found to be significantly decreased in DKA patients compared with controls. Two physiologically relevant CMs were prepared (DKA-CM and CON-CM) on the basis of measurements from five altered analytes (CXCL1, CXCL8, IL-6, IFNα2, and CXCL10, $P < 0.01$ to control for repeated measures; Table 2).

Table 2. *Human plasma cytokine and soluble adhesion molecule concentrations measured in CON and DKA type 1 diabetes patients*

	CON	DKA	Fold Change	*P* Value
IL-6	4.0 ± 1.8	22.0 ± 4.7	5.5	**0.001**
CXCL1 (GROα)	94.4 ± 10.1	203.6 ± 27.2	2.2	**0.003**
CXCL8 (IL-8)	9.2 ± 2.4	43.7 ± 16.6	4.7	**0.005**
CXCL10 (IP-10)	525.2 ± 92.1	169.1 ± 28.1	0.3	**0.004**
IFNα2	28.7 ± 11.2	69.8 ± 25.7	2.4	**0.005**
IL-2	1.3 ± 0.5	4.0 ± 1.0	3.0	0.029
G-CSF	31.6 ± 6.7	96.3 ± 31.9	3.0	0.028
IL-1β	3.1 ± 1.5	2.4 ± 1.6	0.8	0.172
IL-10	42.3 ± 20.8	135.5 ± 75.9	3.2	0.326
IL-17	7.8 ± 4.8	7.7 ± 2.2	1.0	0.082
IFNγ	20.8 ± 9.8	28.1 ± 17.5	1.4	0.545
GM-CSF	65.4 ± 24.0	33.4 ± 7.3	0.5	0.821
VEGF	114.2 ± 56.4	179.3 ± 43.1	1.6	0.137
CCL2 (MCP-1)	336.4 ± 33.4	302.0 ± 43.4	0.9	0.539
CCL3 (MIP-1α)	9.2 ± 1.7	14.6 ± 3.4	1.6	0.184
CCL4 (MIP-1β)	46.9 ± 7.5	52.3 ± 8.7	1.1	0.642
TNFα	10.0 ± 0.8	9.3 ± 1.6	0.9	0.694
sCD40L	577.6 ± 91.2	1,056.0 ± 299.1	1.8	0.131
sE-selectin[a]	61.6 ± 8.6	69.0 ± 8.2	1.1	0.536
sICAM-1[a]	203.7 ± 13.8	185.6 ± 23.4	0.9	0.516
sVCAM-1[a]	1,347.5 ± 63.3	1,232.9 ± 99.8	0.9	0.345

Values are means ± SE; $n = 10$. CXCL, CXC chemokine ligand; GROα, growth-regulated oncogene-α; IP-10, IFNγ-induced protein-10; G-CSF, granulocyte colony-stimulating factor; GM-CSF, granulocyte macrophage colony-stimulating factor; VEGF, vascular endothelial growth factor; CCL2, -3, and -4, CC chemokine ligand 2, 3, and 4, respectively; MCP-1, monocyte chemoattractant protein-1; MIP-1α and -β, macrophage inflammatory protein-1α and -β, respectively; sCD40L, soluble cluster of differentiation 40 ligand; sE-selectin, soluble endothelium-selectin; sICAM, soluble intracellular adhesion molecule-1; sVCAM, soluble vascular cell adhesion molecule-1. To control for repeated measurements, only *P* values <0.01 were considered significant (in boldface). [a]Concentrations are reported in ng/ml for sE-selectin, sICAM, and sVCAM, whereas all the rest are in pg/ml.

Three soluble adhesion molecules (sE-selectin, sICAM-1, and sVCAM-1) were measured in plasma as markers of endothelial activation/injury. DKA did not alter plasma soluble adhesion molecule concentrations relative to type 1 diabetes control patients (Table 2).

DKA-induced oxidative stress in hCMEC/D3 cells. Intracellular oxidative stress, as a consequence of ROS production, is an early marker of vascular endothelial cell activation during inflammation (6, 18). Stimulation of hCMEC/D3 with DKA-P, compared with CON-P, for 1 h resulted in a significant increase in ROS production ($P < 0.01$; Fig. 1*A*). On the contrary, stimulation of hCMEC/D3 cells with DKA-CM for 1 h did not increase oxidative stress (Fig. 1*B*). These data suggest that plasma factors in DKA that are distinct from the altered inflammatory cytokines/chemokines mediate cerebrovascular endothelial oxidative stress.

DKA plasma failed to induce TEER changes in a "static" system. Given the significant increase in hCMEC/D3 ROS elicited by DKA-P, we tested whether DKA-P would alter hCMEC/D3 permeability. Because our experimental "flow" system does not allow for permeability measurements, we could test only the effects of DKA-P under static conditions. Application of DKA-P did not alter TEER relative to CON-P (Fig. 2), suggesting that DKA-P alone was insufficient to alter hCMEC/D3 permeability in the absence of shear stress elicited by flow.

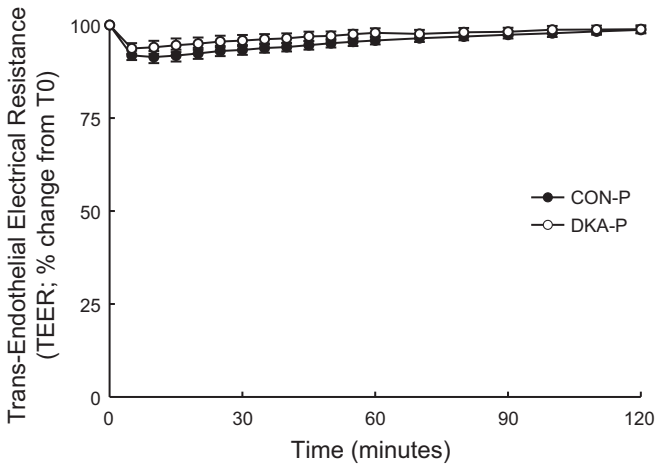

Fig. 2. DKA-P did not decrease transendothelial electric resistance (TEER) of hCMEC/D3 cells under "static" conditions. hCMEC/D3 monolayers were grown on 0.4-μm pore size membranes (Transwell inserts). TEER (Ω) of the hCMEC/D3 monolayer was measured at multiple time points during stimulation with either CON or DKA plasma (20% vol/vol). Results are expressed as %baseline TEER at *time 0* (T_0 min); $n = 10$/group.

DKA-induced a proadhesive phenotype in hCMEC/D3 cells under flow conditions. A common vascular reaction to injury is adhesion of leukocytes to endothelium (16). Stimulation of hCMEC/D3 cells with either DKA-P or DKA-CM for 6 h followed by perfusion of freshly isolated PMNs resulted in significantly increased adhesion compared with controls (plasma $P < 0.01$, CM $P < 0.05$; Fig. 3). Because CXCL1 and CXCL8 are major neutrophil chemoattractants increased in

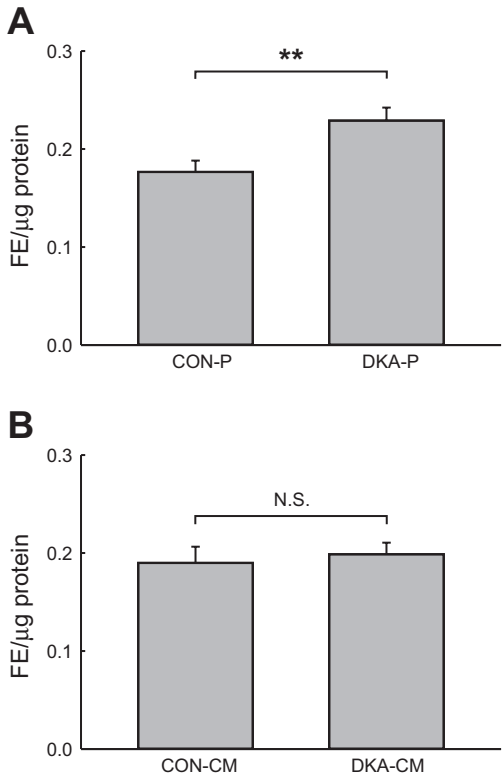

Fig. 1. Diabetic ketoacidosis plasma (DKA-P) induced oxidative stress in hCMEC/D3 cells. Cells were incubated with 10 μM dihydrorhodamine 123 for 45 min prior to stimulation with either 20% plasma (CON-P and DKA-P; *A*) or cytomix (CON-CM and DKA-CM; *B*) for 1 h. Results are shown as fluorescence emission (FE)/μg of protein; $n = 10$/group (*A*) and 5/group (*B*). $^{**}P < 0.01$. NS, not significant.

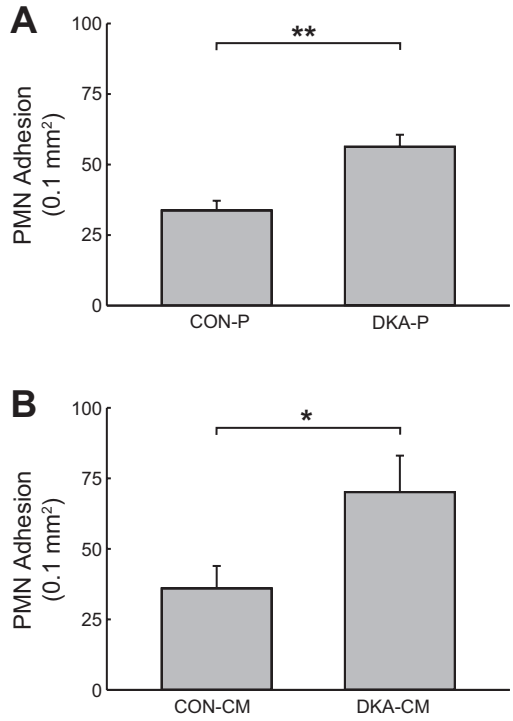

Fig. 3. DKA-P and DKA-CM increased polymorphonuclear leukocyte (PMN) adhesion on hCMEC/D3 cells. Cells were stimulated with 20% control CON-P/DKA-P (*A*) or CON-CM/DKA-CM (*B*) for 6 h prior to PMN perfusion. $^{*}P < 0.05$, $^{**}P < 0.01$; $n = 10$/group (*A*) and 6/group (*B*).

plasma by DKA, we then added 1 μg/ml CXCL1/CXCL8-neutralizing antibodies to either DKA-P or DKA-CM. CXCL1/CXCL8-neutralizing antibodies significantly reduced PMN adhesion to hCMEC/D3 compared with an isotype control (mouse IgG_1, $P < 0.01$; Fig. 4). These results suggest that circulating CXCL1/CXCL8 plays a key role in PMN adhesion to cerebrovascular endothelium in DKA.

To further elucidate the endothelial receptors mediating CXCL1/CXCL8, we incubated hCMEC/D3 with 1 μg/ml of anti-CXCR1/CXCR2 antibodies for 6 h prior to the addition of DKA-P or DKA-CM. CXCR1/CXCR2-neutralizing antibodies significantly suppressed PMN adhesion to hCMEC/D3 compared with the isotype control (mouse IgG2A) (plasma $P < 0.01$, CM $P < 0.05$; Fig. 5). These latter data suggest that the DKA-induced increase of CXCL1/CXCL8 elicited a cerebrovascular endothelium proadhesive phenotype via CXCR1/CXCR2.

As a final experiment, we measured adhesion molecule mRNA expression (E-selectin, ICAM-1, and VCAM-1) in hCMEC/D3 cells stimulated for 4 h (6, 31, 33) with either DKA-P or CON-P. These latter experiments showed that DKA-P failed to alter mRNA expression levels of the three adhesion molecules relative to CON-P (Fig. 6).

DISCUSSION

In the present study, we found altered inflammatory cytokines/chemokines in plasma from pediatric type 1 diabetes with acute DKA and showed that this DKA-induced inflammation was sufficient to instigate leukocyte adhesion to the cerebrovascular endothelium. Leukocyte-endothelial interaction is a key mechanism instigating vascular injury/dysfunction (16). We identified CXCL1/CXCL8 as mediators of human DKA-induced leukocyte-endothelium adhesion via CXCR1/CXCR2. To our knowledge, experiments using human DKA tissues have not been reported previously. Furthermore, the data presented herein may help explain intracranial vascular complications in children with DKA.

DKA elicits a systemic inflammatory response associated with increased blood inflammatory markers (8, 20–22, 25, 27, 35). We report that levels of five cytokines are significantly altered in plasma from children with DKA, including CXCL1 (GROα), CXCL8 (IL-8), IL-6, IFNα2, and CXCL10 (IP-10). Soluble adhesion molecules, including sE-selectin, sICAM-1, and sVCAM-1, were unchanged in plasma by DKA. These data indicate a host cytokine/chemokine reaction to DKA independent of changes in common adhesion molecules (7, 16).

Leukocyte adhesion to the endothelium is a hallmark of inflammation (16). CXC chemokines, including CXCL1 (GROα) and CXCL8, (IL-8) are critical for leukocyte recruitment (28). Circulating levels of CXCL1 were increased significantly in adult type 1 diabetes (47), and CXCL8 is elevated in children with type 1 diabetes (10) and severe/moderate DKA

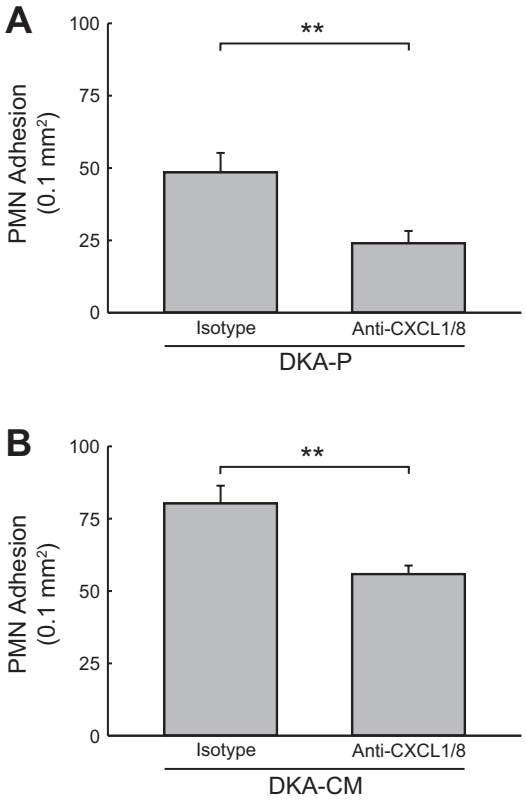

Fig. 4. Anti-CXC chemokine ligand (CXCL)1/CXCL8-neutralizing antibodies suppressed PMN adhesion induced by the stimulation of DKA-P or DKA-CM to hCMEC/D3 cells. Cells were stimulated with 20% DKA-P (*A*) or DKA-CM (*B*) mixed with 1 μg/ml anti-CXCL1 and anti-CXCL8 antibodies or mouse IgG_1 isotype control for 6 h prior to perfusion of PMN. $^{**}P < 0.01$; n = 10/group (*A*) and 5/group (*B*).

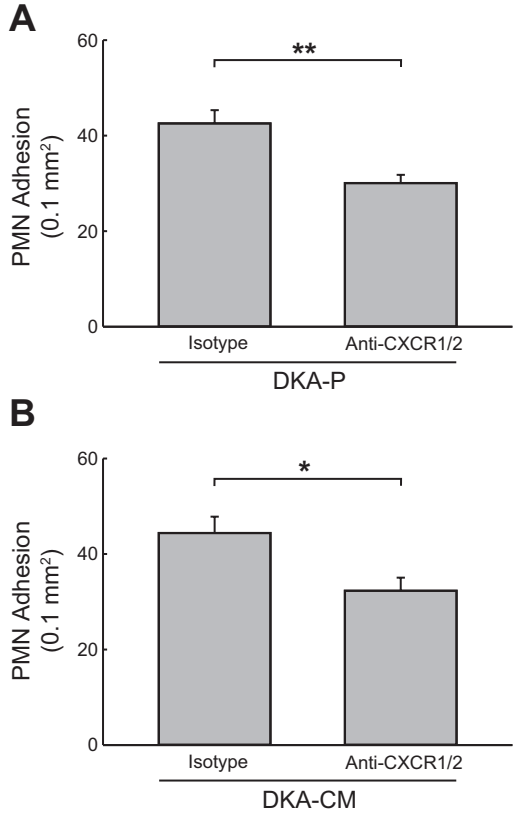

Fig. 5. Blocking CXC chemokine receptor (CXCR)1/CXCR2 on hCMEC/D3 suppressed PMN adhesion induced by the stimulation of DKA-P or DKA-CM to hCMEC/D3 cells. Cells were preincubated with 1 μg/ml anti-CXCR1 and anti-CXCR2 antibodies or mouse IgG_{2A} isotype control for 30 min. Subsequently, 20% DKA-P (*A*) or DKA-CM (*B*) was added to hCMEC/D3 for 6 h prior to perfusion of PMN. $^{*}P < 0.05$, $^{**}P < 0.01$; n = 10/group (*A*) and 7/group (*B*).

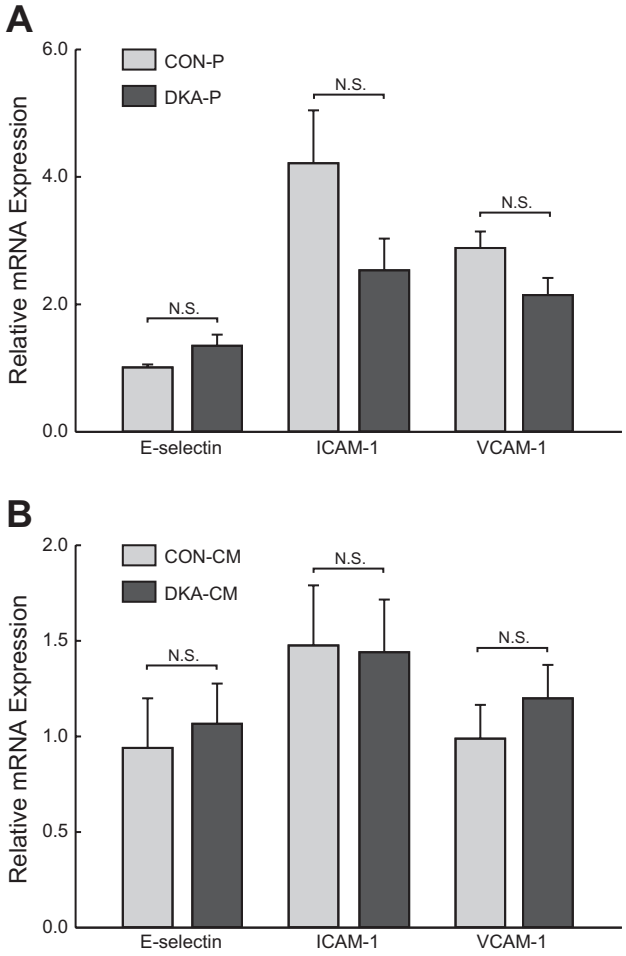

Fig. 6. DKA-P and DKA-CM did not increase expression of E-selectin, intercellular adhesion molecule 1 (ICAM-1), or vascular cell adhesion molecule 1 (VCAM-1) mRNA in hCMEC/D3 cells. Cells were stimulated with 20% CON-P/DKA-P (*A*) or CON-CM/DKA-CM (*B*) for 4 h prior to mRNA isolation. Results are expressed as relative expression compared with the negative control (VL medium alone); $n = 10$/group (*A*) and $n = 5$/group (*B*).

(20, 27). We have shown that CXCL1 and CXCL8 were elevated in children with DKA compared with controlled type 1 diabetes patients and that these two chemokines mediated leukocyte adhesion to hCMEC/D3 via CXCR1/CXCR2.

CXCR1 and CXCR2 are expressed on vascular endothelium and mediate cell proliferation, survival, migration, invasion, and capillary-like structure formation (19, 46). CXCL1 and CXCL8 activate CXCR2, whereas only CXCL8 binds CXCR1 with high affinity (13). CXCL8 is generally more potent as a human neutrophil chemotactic agent and for instigating powerful respiratory bursts in human neutrophils (13, 29), for which the latter may inflict significant injury to the underlying endothelium.

CXCL8 induces the formation of filopodia-like protrusions on endothelial cells, which are mediated by activation of CXCR1/CXCR2. On these mesh structures, the circulating chemokines are presented to PMN by glycosaminoglycan (50), and CXCL8 activates endothelial cell CXCR1 and CXCR2 through Rho and Rac signaling pathways (43). Thus, our data are consistent with circulating CXCL1/CXCL8 activating cerebrovascular endothelial cells through CXCR1/CXCR2, with the reinforcement of chemokine presentation to neutrophils by glycosaminoglycan. CXCL1/CXCL8 mediates adhesion of PMN through the activation of LFA-1 and Mac-1 (45).

In our static Transwell insert system, DKA-P alone failed to alter cerebrovascular endothelial permeability. In contrast, DKA-P induced PMNs to adhere on cerebrovascular endothelium under flow conditions that induce endothelial shear stress. Adhered leukocytes can migrate to the stroma and compromise microvessel integrity, which is associated with a local disruption of the cerebrovascular endothelial cell tight junctions and degradation of basement membrane (16). Cerebrovascular disruption increases permeability, allowing fluid to pass into the brain parenchyma, causing vasogenic edema (24). Compromised microvessels are also prone to platelet adhesion and aggregation that could result in hemorrhage or stroke (12, 34).

In this study, DKA significantly increased IL-6 and IFNα2, whereas CXCL10 was significantly decreased. IL-6 is a proinflammatory cytokine (26) shown previously to be elevated by DKA (20, 27). IFNα, a cytokine that participates in the innate immune response to viral infection (37), has not previously been associated with human DKA. DKA decreased the levels of CXCL10, a chemoattractant for lymphocytes/macrophages (17), suggesting that the primary chemokine response in DKA is neutrophilic (elevated CXCL1/CXCL8).

Oxidative stress markers were elevated in the postmortem brains of two pediatric patients after fatal brain edema associated with DKA (23). Cerebrovascular dysfunction is caused by ROS directly and via tight junction modification and matrix metalloproteinase activation (39). Intracellular ROS accumulates secondary to mitochondrial dysfunction (30, 36). We show that DKA-P, but not DKA-CM, elevated intracellular oxidative stress in hCMEC/D3, indicating that DKA-P contains mitochondrial toxic substances exclusive of alterations in the cytokines/chemokines we investigated. ROS production induced by DKA-P was independent of pH changes, as our experiments were performed at physiological pH due to the pH buffering capability of the culture media. At present, it is unclear how ROS production in cerebrovascular endothelium would be influenced by DKA conditions, as both the intracellular pH and enzymatic activities can vary considerably (44). Oxidative stress at the cerebrovascular endothelium would be additive both from endogenous endothelial production and from adjacent neutrophils stimulated by CXCL1/CXCL8.

Despite the novelty of our study, there are limitations. First, DKA-P was diluted 20% (vol/vol) in the culture media, a dilution necessary to avoid plasma coagulation and maintain hCMEC/D3 monolayer integrity. Because the diluted plasma may have underestimated cytokine/chemokine-mediated effects, we employed cytokine mixtures that were designed to replicate physiological concentrations in plasma. Second, DKA-P was added to culture media that had pH buffering effects and thus did not reproduce the acidic state. Thus, our experiments are selective for DKA-induced inflammatory mediators. Future experiments should investigate mechanisms within a range of pH (i.e., 6.9–7.4) encountered during DKA presentation and correction. Third, in an attempt to replicate the hypovolemic DKA state in our experiments, we used relatively low shear stress (6). Given that the in vivo cerebrovascular shear stress is unknown in DKA and likely evolves between DKA presentation and pH/volume correction, future studies should investigate leukocyte adhesion dynamics with a

range of shear stress (i.e., 0.35–3.5 dynes/cm^2). Fourth, for ethical and practical reasons, we used hCMEC/D3 cells as a model for the cerebrovascular endothelium. Despite the well-characterized properties of the hCMEC/D3 cell line, we cannot definitively conclude that the properties mirror those of a child's developing cerebrovasculature. Fifth, the exact roles of CXCL1 and CXCL8 could not be dissected due to their overlapping actions at CXCR1/CXCR2. Finally, our experiments do not rule out additional autocrine factors that may have been released by DKA-activated cerebrovascular endothelium.

In conclusion, we had demonstrated previously that DKA elicited with pancreatic toxins in a juvenile mouse model produced systemic inflammation associated with cerebrovascular endothelial cell dysfunction (6). In this DKA study, we expanded our mechanistic investigations to human tissues, showing that elevated CXCL1/CXCL8 mediates leukocyte endothelial adhesion, potentially contributing to DKA-associated intracranial vascular complications.

ACKNOWLEDGMENTS

We thank Dr. Carolina Gillio-Meina, Research Associate at the London Translational Research Centre (www.translationalresearch.ca), for assistance with plasma collection. We also thank Dr. Fukashi Serizawa, Christopher Blom, and Claudia Augustine for technical assistance. This article was critically reviewed by members of the Canadian Critical Care Translational Biology Group (www.CCCTBG.ca), Dr. Brent Winston, and Dr. Alison Fox-Robidchaud.

GRANTS

D. D. Fraser was supported by the grants from the Children's Health Foundation (www.childhealth.ca, London, ON, Canada) and the PSI Foundation. G. Cepinskas was supported by the Heart and Stroke Foundation of Ontario (NA6914).

DISCLOSURES

No conflicts of interest, financial or otherwise, are declared by the authors.

AUTHOR CONTRIBUTIONS

T.O., G.C., C.C., E.P., I.A., K.S., P.O.C., I.R., and B.W. performed experiments; T.O., G.C., E.P., K.S., and D.F. analyzed data; T.O., G.C., C.C., E.P., I.A., K.S., P.O.C., I.R., B.W., and D.F. interpreted results of experiments; T.O. and D.F. prepared figures; T.O. drafted manuscript; T.O., G.C., C.C., E.P., I.A., K.S., P.O.C., I.R., B.W., and D.F. edited and revised manuscript; T.O., G.C., C.C., E.P., I.A., K.S., P.O.C., I.R., B.W., and D.F. approved final version of manuscript; T.O., G.C., and D.F. conception and design of research.

REFERENCES

1. **Brisson AR, Matsui D, Rieder MJ, Fraser DD.** Translational research in pediatrics: tissue sampling and biobanking. *Pediatrics* 129: 153–162, 2012.
2. **Cepinskas G, Katada K, Bihari A, Potter RF.** Carbon monoxide liberated from carbon monoxide-releasing molecule CORM-2 attenuates inflammation in the liver of septic mice. *Am J Physiol Gastrointest Liver Physiol* 294: G184–G191, 2008.
3. **Cepinskas G, Lush CW, Kvietys PR.** Anoxia/reoxygenation-induced tolerance with respect to polymorphonuclear leukocyte adhesion to cultured endothelial cells. A nuclear factor-kappaB-mediated phenomenon. *Circ Res* 84: 103–112, 1999.
4. **Chase HP, Garg SK, Jelley DH.** Diabetic ketoacidosis in children and the role of outpatient management. *Pediatr Rev* 11: 297–304, 1990.
5. **Chiasson JL, Aris-Jilwan N, Belanger R, Bertrand S, Beauregard H, Ekoe JM, Fournier H, Havrankova J.** Diagnosis and treatment of diabetic ketoacidosis and the hyperglycemic hyperosmolar state. *CMAJ* 168: 859–866, 2003.
6. **Close TE, Cepinskas G, Omatsu T, Rose KL, Summers K, Patterson EK, Fraser DD.** Diabetic ketoacidosis elicits systemic inflammation associated with cerebrovascular endothelial cell dysfunction. *Microcirculation* 20: 534–543, 2013.
7. **Cotran RS, Mayadas-Norton T** Endothelial adhesion molecules in health and disease. *Pathol Biol (Paris)* 46: 164–170, 1998.
8. **Dalton RR, Hoffman WH, Passmore GG, Martin SL.** Plasma C-reactive protein levels in severe diabetic ketoacidosis. *Ann Clin Lab Sci* 33: 435–442, 2003.
9. **Dunger DB, Sperling MA, Acerini CL, Bohn DJ, Daneman D, Danne TP, Glaser NS, Hanas R, Hintz RL, Levitsky LL, Savage MO, Tasker RC, Wolfsdorf JI.** ESPE/LWPES consensus statement on diabetic ketoacidosis in children and adolescents. *Arch Dis Child* 89: 188–194, 2004.
10. **Erbagci AB, Tarakcioglu M, Coskun Y, Sivasli E, Sibel Namiduru E.** Mediators of inflammation in children with type I diabetes mellitus: cytokines in type I diabetic children. *Clin Biochem* 34: 645–650, 2001.
11. **Figueroa RE, Hoffman WH, Momin Z, Pancholy A, Passmore GG, Allison J.** Study of subclinical cerebral edema in diabetic ketoacidosis by magnetic resonance imaging T2 relaxometry and apparent diffusion coefficient maps. *Endocr Res* 31: 345–355, 2005.
12. **Foster JR, Morrison G, Fraser DD.** Diabetic ketoacidosis-associated stroke in children and youth. *Stroke Res Treat* 2011: 219706, 2011.
13. **Geiser T, Dewald B, Ehrengruber MU, Clark-Lewis I, Baggiolini M.** The interleukin-8-related chemotactic cytokines GRO alpha, GRO beta, and GRO gamma activate human neutrophil and basophil leukocytes. *J Biol Chem* 268: 15419–15424, 1993.
14. **Gillio-Meina C, Cepinskas G, Cecchini EL, Fraser DD.** Translational research in pediatrics II: blood Collection, processing, shipping, and storage. *Pediatrics* 131: 754–766, 2013.
15. **Glaser NS, Wootton-Gorges SL, Marcin JP, Buonocore MH, Dicarlo J, Neely EK, Barnes P, Bottomly J, Kuppermann N.** Mechanism of cerebral edema in children with diabetic ketoacidosis. *J Pediatr* 145: 164–171, 2004.
16. **Granger DN, Senchenkova E.** Inflammation and the microcirculation. In: *Integrated Systems Physiology: From Molecule to Function*. San Rafael, CA: Morgan & Claypool Life Sciences Publishers, 2010, vol. 2, no. 1, p. 1–87.
17. **Groom JR, Luster AD.** CXCR3 ligands: redundant, collaborative and antagonistic functions. *Immunol Cell Biol* 89: 207–215, 2011.
18. **Handa O, Stephen J, Cepinskas G.** Role of endothelial nitric oxide synthase-derived nitric oxide in activation and dysfunction of cerebrovascular endothelial cells during early onsets of sepsis. *Am J Physiol Heart Circ Physiol* 295: H1712–H1719, 2008.
19. **Hillyer P, Mordelet E, Flynn G, Male D.** Chemokines, chemokine receptors and adhesion molecules on different human endothelia: discriminating the tissue-specific functions that affect leucocyte migration. *Clin Exp Immunol* 134: 431–441, 2003.
20. **Hoffman WH, Burek CL, Waller JL, Fisher LE, Khichi M, Mellick LB.** Cytokine response to diabetic ketoacidosis and its treatment. *Clin Immunol* 108: 175–181, 2003.
21. **Hoffman WH, Casanova MF, Cudrici CD, Zakranskaia E, Venugopalan R, Nag S, Oglesbee MJ, Rus H.** Neuroinflammatory response of the choroid plexus epithelium in fatal diabetic ketoacidosis. *Exp Mol Pathol* 83: 65–72, 2007.
22. **Hoffman WH, Helman SW, Passmore G.** Acute activation of peripheral lymphocytes during treatment of diabetic ketoacidosis. *J Diabetes Complications* 15: 144–149, 2001.
23. **Hoffman WH, Siedlak SL, Wang Y, Castellani RJ, Smith MA.** Oxidative damage is present in the fatal brain edema of diabetic ketoacidosis. *Brain Res* 1369: 194–202, 2011.
24. **Hoffman WH, Stamatovic SM, Andjelkovic AV.** Inflammatory mediators and blood brain barrier disruption in fatal brain edema of diabetic ketoacidosis. *Brain Res* 1254: 138–148, 2009.
25. **Jerath RS, Burek CL, Hoffman WH, Passmore GG.** Complement activation in diabetic ketoacidosis and its treatment. *Clin Immunol* 116: 11–17, 2005.
26. **Kamimura D, Ishihara K, Hirano T.** IL-6 signal transduction and its physiological roles: the signal orchestration model. *Rev Physiol Biochem Pharmacol* 149: 1–38, 2003.
27. **Karavanaki K, Karanika E, Georga S, Bartzeliotou A, Tsouvalas M, Konstantopoulos I, Fotinou A, Papassotiriou I, Karayianni C.** Cytokine response to diabetic ketoacidosis (DKA) in children with type 1 diabetes (T1DM). *Endocr J* 58: 1045–1053, 2011.
28. **Kobayashi Y.** The role of chemokines in neutrophil biology. *Front Biosci* 13: 2400–2407, 2008.

29. **L'Heureux GP, Bourgoin S, Jean N, McColl SR, Naccache PH.** Diverging signal transduction pathways activated by interleukin-8 and related chemokines in human neutrophils: interleukin-8, but not NAP-2 or GRO alpha, stimulates phospholipase D activity. *Blood* 85: 522–531, 1995.
30. **Lenaz G.** Mitochondria and reactive oxygen species. Which role in physiology and pathology? *Adv Exp Med Biol* 942: 93–136, 2012.
31. **Ley K, Reutershan J.** Leucocyte-endothelial interactions in health and disease. *Handb Exp Pharmacol*: 97–133, 2006.
32. **Lin JJ, Lin KL, Wang HS, Wong AM, Hsia SH.** Occult infarct with acute hemorrhagic stroke in juvenile diabetic ketoacidosis. *Brain Dev* 30: 91–93, 2008.
33. **Lush CW, Kvietys PR.** Microvascular dysfunction in sepsis. *Microcirculation* 7: 83–101, 2000.
34. **Mahmud FH, Ramsay DA, Levin SD, Singh RN, Kotylak T, Fraser DD.** Coma with diffuse white matter hemorrhages in juvenile diabetic ketoacidosis. *Pediatrics* 120: e1540–e1546, 2007.
35. **Oglesbee MJ, Herdman AV, Passmore GG, Hoffman WH.** Diabetic ketoacidosis increases extracellular levels of the major inducible 70-kDa heat shock protein. *Clin Biochem* 38: 900–904, 2005.
36. **Omatsu T, Naito Y, Handa O, Mizushima K, Hayashi N, Qin Y, Harusato A, Hirata I, Kishimoto E, Okada H, Uchiyama K, Ishikawa T, Takagi T, Yagi N, Kokura S, Ichikawa H, Yoshikawa T.** Reactive oxygen species-quenching and anti-apoptotic effect of polaprezinc on indomethacin-induced small intestinal epithelial cell injury. *J Gastroenterol* 45: 692–702, 2010.
37. **Pestka S, Krause CD, Walter MR.** Interferons, interferon-like cytokines, and their receptors. *Immunol Rev* 202: 8–32, 2004.
38. **Pinkey JH, Bingley PJ, Sawtell PA, Dunger DB, Gale EA.** Presentation and progress of childhood diabetes mellitus: a prospective population-based study. The Bart's-Oxford Study Group. *Diabetologia* 37: 70–74, 1994.
39. **Pun PB, Lu J, Moochhala S.** Involvement of ROS in BBB dysfunction. *Free Radic Res* 43: 348–364, 2009.
40. **Roe TF, Crawford TO, Huff KR, Costin G, Kaufman FR, Nelson MD Jr.** Brain infarction in children with diabetic ketoacidosis. *J Diabetes Complications* 10: 100–108, 1996.
41. **Rose KL, Pin CL, Wang R, Fraser DD.** Combined insulin and bicarbonate therapy elicits cerebral edema in a juvenile mouse model of diabetic ketoacidosis. *Pediatr Res* 61: 301–306, 2007.
42. **Rosenbloom AL, Schatz DA, Krischer JP, Skyler JS, Becker DJ, Laporte RE, Libman I, Pietropaolo M, Dosch HM, Finberg L, Muir A, Tamborlane WV, Grey M, Silverstein JH, Malone JI.** Therapeutic controversy: prevention and treatment of diabetes in children. *J Clin Endocrinol Metab* 85: 494–522, 2000.
43. **Schraufstatter IU, Chung J, Burger M.** IL-8 activates endothelial cell CXCR1 and CXCR2 through Rho and Rac signaling pathways. *Am J Physiol Lung Cell Mol Physiol* 280: L1094–L1103, 2001.
44. **Schulz E, Munzel T.** Intracellular pH: a fundamental modulator of vascular function. *Circulation* 124: 1806–1807, 2011.
45. **Seo SM, McIntire LV, Smith CW.** Effects of IL-8, Gro-α, and LTB_4 on the adhesive kinetics of LFA-1 and Mac-1 on human neutrophils. *Am J Physiol Cell Physiol* 281: C1568–C1578, 2001.
46. **Singh S, Wu S, Varney M, Singh AP, Singh RK.** CXCR1 and CXCR2 silencing modulates CXCL8-dependent endothelial cell proliferation, migration and capillary-like structure formation. *Microvasc Res* 82: 318–325, 2011.
47. **Takahashi K, Ohara M, Sasai T, Homma H, Nagasawa K, Takahashi T, Yamashina M, Ishii M, Fujiwara F, Kajiwara T, Taneichi H, Takebe N, Satoh J.** Serum CXCL1 concentrations are elevated in type 1 diabetes mellitus, possibly reflecting activity of anti-islet autoimmune activity. *Diabetes Metab Res Rev* 27: 830–833, 2011.
48. **Weksler B, Romero IA, Couraud PO.** The hCMEC/D3 cell line as a model of the human blood brain barrier. *Fluids Barriers CNS* 10: 16, 2013.
49. **Weksler BB, Subileau EA, Perriere N, Charneau P, Holloway K, Leveque M, Tricoire-Leignel H, Nicotra A, Bourdoulous S, Turowski P, Male DK, Roux F, Greenwood J, Romero IA, Couraud PO.** Blood-brain barrier-specific properties of a human adult brain endothelial cell line. *FASEB J* 19: 1872–1874, 2005.
50. **Whittall C, Kehoe O, King S, Rot A, Patterson A, Middleton J.** A chemokine self-presentation mechanism involving formation of endothelial surface microstructures. *J Immunol* 190: 1725–1736, 2013.